

**In Silico insight of Cystic Fibrosis and its invitro diagnostic potential using
Karakoram clay extracted Silica Nanoparticles**



By

Anza Faheem (239363)

Muhammad Talha Basir (240014)

Pakiza Riasat (240185)

Tehrim Naveed (240296)

Thesis Supervisor: **Dr. Shah Rukh Abbas**

Atta-ur-Rahman School of Applied Biosciences

National University of Sciences and Technology (NUST)

Islamabad, Pakistan

(2021)

THESIS ACCEPTANCE CERTIFICATE

Certified that the contents and form of thesis entitled “**In Silico insights of Cystic Fibrosis and its invitro diagnostic potential using Karakoram clay extracted Silica Nanoparticles**” submitted by UG students Anza Faheem, Muhammad Talha Basir, Pakiza Riasat, and Tehrim Naveed, have been found satisfactory for the requirement of the degree.

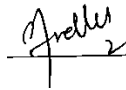
Signature (Supervisor):



Dr. Shah Rukh Abbas

ASAB, NUST

Signature (Head of the Department):

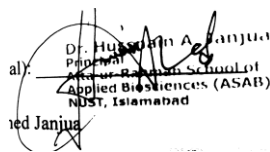


Dr. Saadia Andleeb
Head of Department (h.o.D)
Dept. of Industrial Biotechnology
Asta-ur-Rahman School of Applied
Biosciences (ASAB), NUST Islamabad

Dr. Sadia Andaleeb

ASAB, NUST

Signature (Principal):



Dr. Hussnain A. Janjua
Principal
Asta-ur-Rahman School of
Applied Biosciences (ASAB)
NUST, Islamabad

Dr. Hussnain Ahmed Janjua

ASAB, NUST

Date: 30th June, 2021

AUTHOR'S DECLARATION

We, Anza Faheem, Muhammad Talha Basir, Pakiza Riasat, and Tehrim Naveed, hereby state that our BS FYP thesis titled “In Silico insights of Cystic Fibrosis and its invitro diagnostic potential using Karakoram clay extracted Silica Nanoparticles” is our own work and has not been submitted previously by us for taking any degree from this university National University of Sciences and Technology (NUST) or anywhere else in the country/world.

At any time if our statement is found to be incorrect even after my graduation, the university has the right to withdraw our BS degree.

Student name: Anza Faheem

Signature:



Student name: M. Talha Basir

Signature:



Student name: Pakiza Riasat

Signature:



Student name: Tehrim Naveed

Signature:



Date: 30th June, 2021

CERTIFICATE FOR PLAGIARISM

It is to confirm that this BS thesis titled “In Silico insights of Cystic Fibrosis and its invitro diagnostic potential using Karakoram clay extracted Silica Nanoparticles” by Anza Faheem (239363), Muhammad Talha Basir (240014), Pakiza Riasat (240185), and Tehrim Naveed (240296) has been examined by me. I undertake that,

1. The thesis has significant new work/knowledge as compared to already published elsewhere. No sentence, table, equation, diagram, paragraph, or section has copied verbatim from previous work except when placed under quotation marks and duly referenced.
2. The work presented is original and own work of authors i.e. there is no plagiarism. No idea, results, or works of others have been presented as authors’ own work.

There is no fabrication of data or results such that the research is not accurately represented in the records. The thesis has been checked using Turnitin, a copy of the originality report attached and focused within limits as per HEC plagiarism policy and instructions.



(Supervisor)

Dr. Shah Rukh Abbas

Assistant Professor

ASAB, NUST

*Dedicated to our all our friends, family, faculty,
and anyone who aims to seek knowledge. May
you all be blessed!*

ACKNOWLEDGEMENTS

We are thankful to our parents for their constant support and prayers. We would also like to thank our principal Dr. Hussnain Janjua for providing us this opportunity, our HoD Dr. Sadia Andleeb, and our supervisor, Dr. Sharukh Abbas for her guidance at every step and her trust in our abilities which made us work on this project confidently.

We are grateful to Mr Zafar (SCME) and Mr Noman (SCME) for their cooperation and allowing us to utilize their labs.

We would also like to thank Iqra Riaz, Muhammad Ali, MS student Shaheer Shafiq, and PhD student Ramish Riaz who helped us throughout the project.

Contents

Abstract.....	1
Introduction.....	2
1.1 Cystic Fibrosis.....	3
1.2 Cystic Fibrosis Transmembrane Conductance Regulator	4
1.2.1 Pore formation	5
1.2.2 Anions inside the pore.....	6
1.3 Composition of Karakoram Clay	7
Literature Review.....	8
2.1 Mutations	9
2.1.1 Classes of Mutation	9
2.2 Drugs.....	10
2.2.1 Ivacaftor	10
2.2.2 Elexacaftor	11
2.2.3 Tezacaftor	11
2.3 Methods for Diagnosing Cystic Fibrosis.....	12
2.3.1 Chloridometer (Titration)	12
2.3.2 Chromogenic Anion Sensors.....	13
2.3.3 FRET Flow Cytometry.....	13
2.3.4 Electrochemical Chloride Quantification.....	13
2.4 Use of Nanotechnology in Diagnostics	14
2.5 Silica Nanoparticles (SiO ₂).....	15
2.5.1 Physicochemical properties.....	15
2.5.2 Drug delivery through SiNPs.....	16
2.5.3 Adsorption	16
2.6 Rationale.....	17
2.7 Aims and Objectives	17

Materials and Methods	18
3.1 Software and programs	19
3.2 Preparation of ligand structures for Ivacaftor, Elexacaftor and Tezacaftor	19
3.3 Preparation of protein structure for Cystic Fibrosis Transmembrane Conductance Regulator (CFTR)	19
3.4 Docking Protocol.....	20
3.5 Post-Docking analyses	21
3.6 Synthesis of Silica Nanoparticles (SiNPs)	22
3.7 Characterization.....	25
3.7.1 Scanning Electron Microscopy (SEM)	25
3.7.2 Fourier-Transform Infra-red Spectroscopy.....	26
3.8 Adsorption of chloride ions	26
Results and Discussions	29
4.1 Docking	30
4.1.1 Wild-type protein-drug interaction	30
4.1.2 Mutant protein-drug interaction.....	30
4.2 Post-docking Analysis	32
4.3 Synthesis of Silica nanoparticles	35
4.4 Characterisation.....	35
4.4.1 SEM	35
4.4.2 FTIR Spectrum.....	37
4.5 Adsorption	38
Conclusion and Future prospects	40
References	42

Table of Figures:

Figure 1: Domain structure of CFTR protein ^[2]	4
Figure 2: CFTR schematic structure ^[3]	5
Figure 3: CFTR Pore model ^[2]	6
Figure 4: Classes of CFTR mutation ^[9]	10
Figure 5: Mutant 6MSM CFTR with K95Q mutation	20
Figure 7: 6MSM CFTR with a highlighted pocket	21
Figure 6: Grid coordinates and grid size	21
Figure 8: Visualization of protein-ligand interaction in PyMol.....	22
Figure 9: Intermolecular interactions in PLIP	22
Figure 10: Clay placed in muffle furnace	24
Figure 11: Clay dissolving in HCl	24
Figure 12: NaOH treated clay being filtered	25
Figure 13: Titration	27
Figure 14: white precipitates	28
Figure 15: drugs in wild and mutant CFTR	34
Figure 16: Silica nanoparticles' pellet	35
Figure 17: SEM images with measurements	36
Figure 18: SEM images of SiNPs	37
Figure 19: FTIR spectrum	38
Figure 20: End point of titration	39

List of Tables

Table 1: Composition of clay	7
Table 2: Physicochemical properties of Drugs	12
Table 3 Chemical composition of Silica	15
Table 4 Physicochemical Properties of silica	15
Table 5: Chemicals and Equipment	23
Table 6: Binding affinities of ivacaftor, elexacaftor and tezacaftor at the binding sites of wildtype CFTR pocket.	30
Table 7: Binding affinities of ivacaftor, elexacaftor and tezacaftor at the binding sites of mutant CFTR pocket.	31
Table 8: Interactions of ivacaftor, elexacaftor and tezacaftor at the binding sites of wildtype CFTR pocket.	32
Table 9: Interactions of ivacaftor, elexacaftor and tezacaftor at the binding sites of wildtype CFTR pocket.	33
Table 10: Cl-1 calculated after titration	39

List of abbreviation

CF	Cystic Fibrosis
CFTR	Cystic Fibrosis Transmembrane Conductance Regulator
ABC	Member Atp-Binding
TMD	Transmembrane Domains
MSD	Membrane Spanning Domains
NBD	Nucleotide Binding Domain
PkA	Protein Kinase A
PkC	Protein Kinase C
SSS	Sodium Silicate Solution
R334	Arginine 334
F337	Phenylalanine337
SiNPs	Silica Nanoparticles
FRET	Förster Resonance Energy Transfer
SEM	Scanning Electron Microscope
FTIR	Fourier Transform Infrared

Abstract

Cystic fibrosis is life threatening hereditary disorder in which the chloride channels present in membrane becomes dysfunctional. Cystic fibrosis transmembrane conductance regulator genes produce CFTR protein that is responsible for the transport of chloride and sodium ion across the membranes. CFTR consist of multiple domains i.e., transmembrane domain, nucleotide binding domains and regulatory domain. There are multiple Mutations in CFTR gene lead to the defective ion exchange affecting the multiple organs.

The K95Q mutation in the CFTR is a Class IV mutation which is characterized by reduced chloride conduction across the membrane. Three FDA approved drugs Ivacaftor, Tezacaftor and Elexacaftor, that are being used for the treatment of G551D and F508 mutations, are selected as a possible treatment for K95Q mutation. Bioinformatics and computational software were used for the molecular docking, visualization, and analysis of the drug ligands interactions with both wildtype and mutant CFTR with K95Q mutation.

Furthermore, silica nanoparticles were extracted from Karakoram clay in order to get some insight into their diagnostic potential. They were characterized through SEM and FTIR. Silica solution was then mixed with NaCl solution to determine the adsorptive properties of SiNPs. The amount of Chloride ions adsorbed was later determined through titration and the results demonstrated that SiNPs have the capacity to adsorb chloride ions to themselves making it possible for them to be used in diagnostic tools for CF and even in drug delivery of the drugs observed in our in silico studies.

Chapter 1:

Introduction

1 Introduction

The booming research in nanotechnology has enabled us to discover and synthesize new varieties of nanomaterials, each possessing its unique set of characteristics. Some of the nanoparticles are associated with optics, electronics, medicine, agriculture, diagnostics, and devices, etc. These nanoparticles are considered to be less cytotoxic and biocompatible due to which they are believed to be the future of medical research and diagnostics. Nanoparticles are currently used for bio-sensing, bio-imaging, and even drug delivery techniques due to their nano-size and extraordinary detecting capabilities.

In our project, we not only studied the *in silico* insights of Cystic Fibrosis (CF) but also synthesized and characterized silica nanoparticles from Karakoram clay along with their diagnostic potential. The *in silico* insight is based on different drug interactions with wild type and mutated Cystic Fibrosis Transmembrane Conductance Regulator (CFTR) protein. While the *in vitro* diagnosis is based on the adsorption and sensitivity of silica nanoparticles towards chloride ions that are present in excess in the sweat sample of a cystic fibrosis patient.

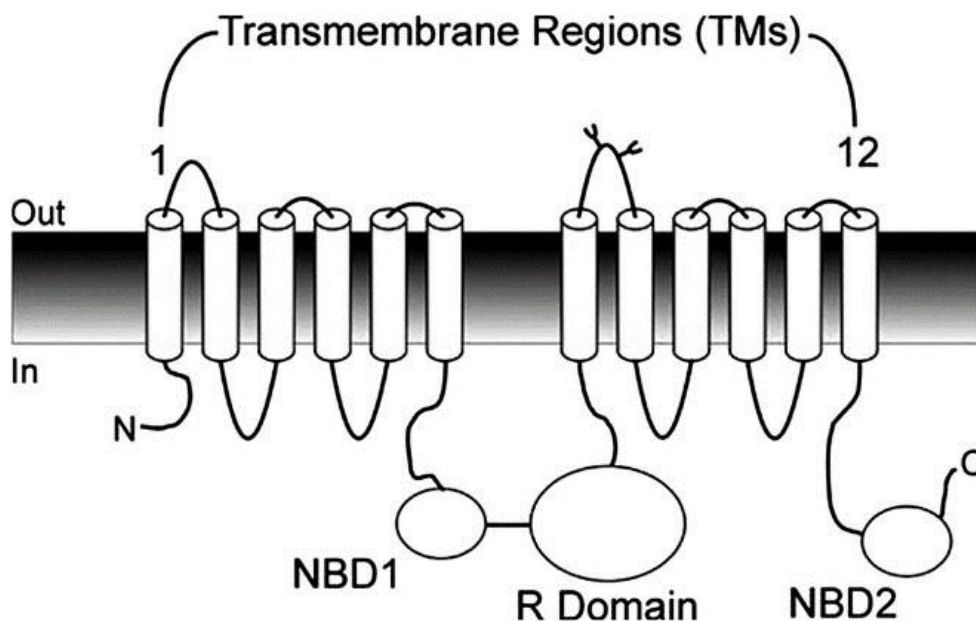
1.1 Cystic Fibrosis

Cystic fibrosis is a complex autosomal recessive disease affecting multiple organ system. It targets digestive, respiratory, reproductive system and sweat gland. However, the most targeted organs of this disease are lungs and digestive system^[1]. In the United States around 1000 new cystic fibrosis case are reported every year majorly affecting the white population. Although it majorly affects Caucasian population, cystic fibrosis is also increasing in nonwhite population. It is fatal disease and lungs complications are major cause of mortality. However, rapid, and early diagnosis help in survival of patients that are suffering from it.

Movement of chloride and sodium ion across the cell membrane is regulated by CFTR protein produced by CFTR genes. When mutation occurs in CFTR gene, there comes a defect in this transport and thick mucus builds in the whole body which leads to respiratory insufficiency. Many bacteria colonize because of the mucus, causing the inflammatory response. This can lead to the destruction of airway and eventually death.

1.2 Cystic Fibrosis Transmembrane Conductance Regulator

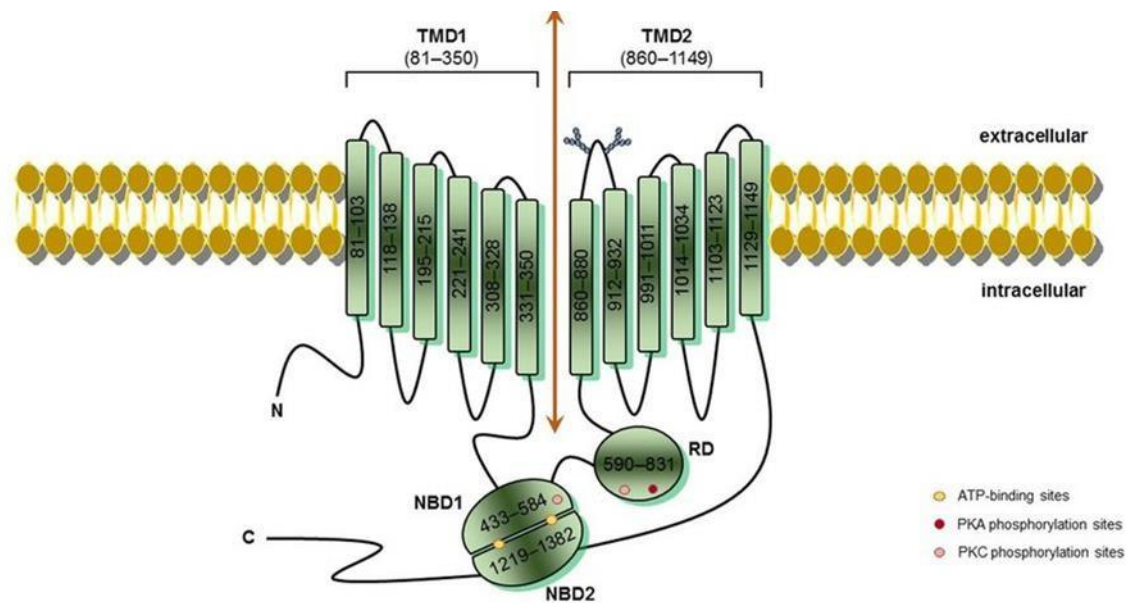
Cystic fibrosis is caused by mutation in cystic fibrosis transmembrane conductance regulator (CFTR) gene, located on chromosome 7, which affects the function of protein it makes i.e., CFTR protein. It is a member ATP-binding cassette (ABC) transporter functioning as a channel that regulate the transport of chloride ion in epithelial cell. It consists of 1480 amino acids and contains 5 domains. There are two transmembrane domains (TMDs) also named as membrane spanning domain (MSD), each of which has six alpha helices that span the membrane. These alpha helices then connect to the nucleotide binding domain 1 (NBD1) present in the cytoplasm. There is another important domain named as regulatory domain (R Domain) that joins it with transmembrane domain 2 which then binds to nucleotide binding domain 2 (NBD2).



[2]
Figure 1: Domain structure of CFTR protein

In case of ABC transporter, G protein receptor is coupled to the G protein which has $G\alpha$, $G\beta$ and $G\gamma$ subunits. Alpha subunit is bound to GDP. When agonist binds to the receptor, there is a transformational change and GDP gets dissociated from the α subunit and GTP binds there, resulting in the activation of G protein. This releases the GTP and alpha subunit from $g\beta$ and $g\gamma$ dimer. The activate GTP- α subunits activates the adenylyl cyclase enzyme present in the membrane. Adenylyl cyclase enzyme converts ATP to cAMP. This cAMP activates protein

kinase A (pkA). Protein kinase C (pkC) comes along with pkA. This pkC phosphorylates the R domain of cystic fibrosis which brings conformational changes in regulatory domains and creates a phosphorylation site for protein kinase A. ATP binds to the nucleotide binding domain 1, as a result of which NBD2 comes closer to NBD1. Consequently, a weak heterodimer of NBD1-NBD2 is formed. This weak bond is converted to the strong heterodimer once second ATP binds to NBD2. This brings transmembrane domain 1 and transmembrane domain 2 closer to each other and ion channel is activated, forming a funnel like structure which opens, and ions pass through it.



[3]
Figure 2: CFTR schematic structure

1.2.1 Pore formation

It has been suggested that transmembrane 1 and 6 play a crucial and major role in the pore formation. Whereas TM5 plays less significant role and TM2, TM3 and TM4 showed no evidence of direct function in forming the pore.

Various studies have shown that there are positively charged Arginine (R334) is present in TM6. These amino acids attract the chloride ion into the pore from extracellular solution whereas, another positive charged amino acid Lysine (K95) in TM1 attracts the chloride ion from intracellular side of the membrane. These positive charges are removed. Consequently,

the rate through which chloride ions enter into the pore decreases significantly, highlighting their importance in the regulation of chloride ions.

1.2.2 Anions inside the pore

Studies show that movement of different ions is coupled to one another suggesting that ions, instead of passing independently through the pore, influence each other's movement. When one anion enters into the pore, it accelerates the exit of already bound ion in the pore. ^[4] When there are multiple chloride ion present in the pore, they experience mutual electrostatic repulsion effect against each other. It accelerates their exit from the pore.

R334 present in the TM6 attracts the chloride ion from extracellular solution and K95 in TM1 attracts chloride ion from intracellular solution. Large anions are also attracted by K95. These larger sized anions will obstruct chloride ion. The F337 and T337 will be present in the central region. Positive charge K95 in TM1 and R334 in TM6 line the narrow central regions forcing chloride ion to move out of the pore.

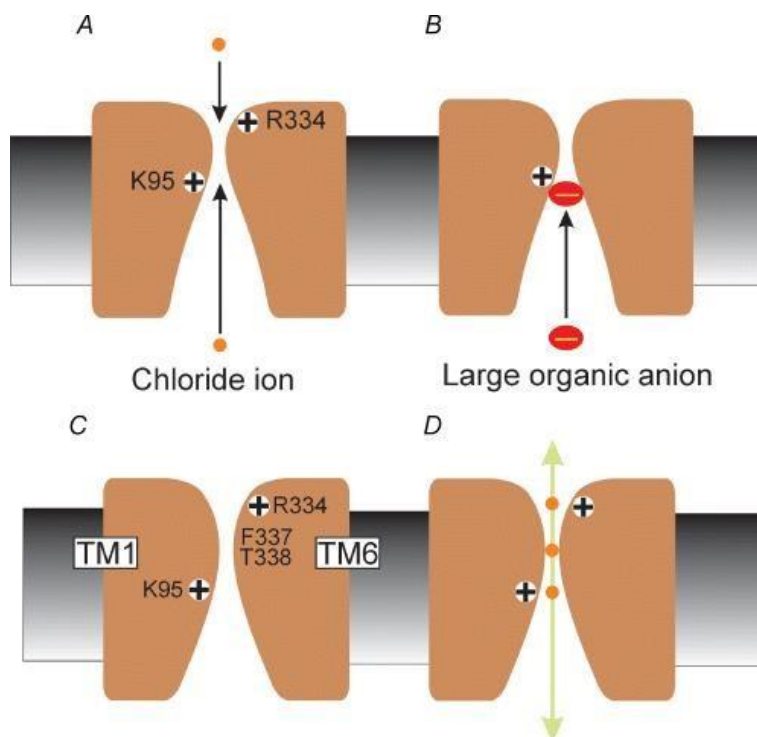


Figure 3: CFTR Pore model ^[2]

1.3 Composition of Karakoram Clay

Silica nanoparticles were extracted from clay, which was obtained from the Karakoram Range, Gilgit-Baltistan. The extreme climate and environment of the range make it very likely that the clay obtained from there would have very unique properties which can be further explored. Plasticity of clay is its most crucial characteristic which is provided by the high content of clay minerals. Hydrous aluminium phyllosilicate minerals, commonly known as clay minerals contain bonds of aluminium and silicon ions formed through the interconnection of oxygen and hydroxyl ions.^[5] The composition of clay is most commonly determined by X-ray diffraction (XRD). The main components of clay are 58.1% SiO₂ and 15.1% Al₂O₃. MgO, K₂O, CaO and TiO₂ are some of the other minerals occurring in smaller amounts.

Chemical Oxide	Weight (%)
SiO ₂	58.10
Al ₂ O ₃	15.10
MgO	2.70
K ₂ O	1.83
TiO ₂	0.88
CaO	0.36

Table 1: Composition of clay

Chapter 2

Literature Review

2 LITERATURE REVIEW

2.1 Mutations

There are over 1600 CFTR mutations that affect the production and function of CFTR protein through different molecular mechanism. Mutations can be classified according to the mechanism by which they affect the function of CFTR protein. Once mechanism of mutation is understood, it provides the basis for discovery of drugs targeted against particular mutations of CFTR.^[6]

2.1.1 Classes of Mutation

In this case of class 1 mutation, there are premature stop codon present, as a result of which unstable RNA is produced or dysfunctional proteins which degrades before reaching to membrane are produced. These are nonsense mutation most of the time. Individuals have class 1 mutant do not have Functional CFTR. W1282X is one of the most common mutations that account for 64% of all the alleles it causes severe symptoms.

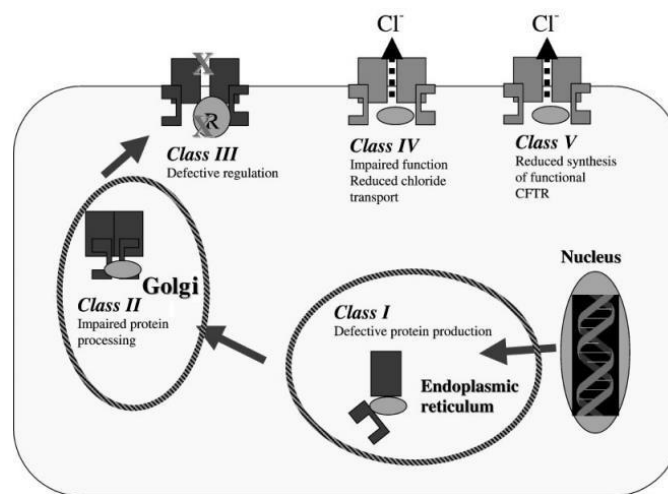
After translation CFTR undergoes through some processes of Glycosylation and folding in Golgi apparatus and Endoplasmic Reticulum. After that, CFTR is then transported to cell membrane. Class 2 affects this process. Three base pair deletion is the most common CFTR mutation that results in the deletion of phenylalanine at position 508. This is the most common type of mutation and accounts for almost 70% of affected allele. As a result, a protein is made that is unable to fold properly. Hence, the faulty protein is kept in Endoplasmic Reticulum and degraded. Misfolded proteins are recognized by Quality control mechanism in Endoplasmic Reticulum and their deployment is blocked by targeting them for degradation. Scientist suggested that if condition is created in which DF508 can exit the ER and reach the surface of cell, it can function as cAMP-dependent chloride channel and correct the cystic fibrosis partially.

CFTR activity is regulated by its phosphorylation by protein kinase A. ATP binds to nucleotide binding domains once the R domain is phosphorylated and chloride ions are moved across the membrane. In class 3 mutation CFTR is produced, processed, and transported but the CFTR produced cannot be phosphorylated. Glycine at codon 551 is

converted to aspartic acid (G551D). Being the third most common mutation, it has frequency of 3.1% among cystic fibrosis chromosomes.^[7]

The individuals with 4th type mutation have CFTR processed and inserted in the apical membranes, but its phosphorylation results in reduced chloride ion conductance. And they have milder cystic fibrosis phenotype. R334, R117H, K95Q are class 4 mutation that reduce the conductance of chloride ion ^[8]

In this mutation the CFTR protein made is not enough in number. Sometimes the incorrect versions of protein are made more than the correct ones and they do not make to the cell surface. Consequently, enough CFTR proteins are not present on the cell membrane.



ⁱ[9]

Figure 4:Classes of CFTR mutation

2.2 Drugs

There are different drugs used for the treatment of cystic Fibrosis. Few of FDA approved drugs are mentioned below.

2.2.1 Ivacaftor

Ivacaftor, known by brand name Kalydeco, is CFTR potentiator. It can be used alone or in combined forms to treat individuals suffering from cystic fibrosis against specific mutations.

Ivacaftor works by keeping the gates open for longer periods of time which helps the transport of ion and water in and out of the cell and clears mucus. The U.S food and Drug Authority (FDA) first approved ivacaftor in 2012 for the cystic fibrosis with G551D mutation only. 5 years later in 2017, FDA approved it for other mutations too.

2.2.2 Elexacaftor

Elexacaftor is next generation corrector cystic fibrosis. It is called next generation because it has different structure and properties as compared to first generation drug. It is used in combination with other drugs; tezacaftor and ivacaftor. These drugs work in a synergistic manner. Elexacaftor facilitates the trafficking of CFTR protein to the cell surface. this increases the mature CFTR on cell surface. FDA approved elexacaftor as combination drug in October 2019.

2.2.3 Tezacaftor

It functions to facilitate the folding of mature CFTR to the cell surface. When tezacaftor combines with elexacaftor and ivacaftor is used for the treatment of cystic fibrosis that has at least one 508 mutations. This improves the protein function for F508 mutation. This drug received its approval on Feb 12, 2018.

Physical properties	Ivacaftor	Elexacaftor	Tezacaftor
PubChem CID	16220172	134587348	46199646
Hydrogen bond donors count	3	1	4
Hydrogen Bond acceptor count	4	11	9
Molecular Formula	$C_{24}H_{28}N_2O_3$	$C_{26}H_{34}F_3N_7O_4S$	$C_{26}H_{27}F_3N_2O_6$
Molecular Weight	392.5	597.7	520.5

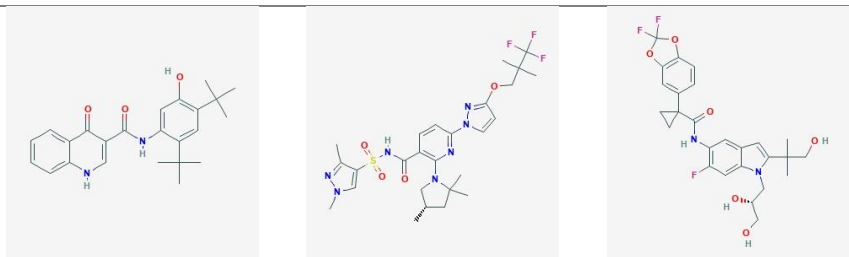
Structure

Table 2: Physicochemical properties of Drugs

2.3 Methods for Diagnosing Cystic Fibrosis

Mutated CFTR gene can be used in the diagnosis of CF through different genetic testing techniques even in the prenatal stage. Different procedures are used to extract a sample of the amniotic fluid or placental tissue and the cells inside these samples are screened for genetic mutations. However, **sweat test** is considered the most prime and standard test for the diagnosis of CF. The levels of electrolytes in the sweat are measured in this test. The levels of sodium and chloride are significantly increased in the CF patients. The concentrations of the ions in adult CF patients are reported to be 60 mmol/L whereas for infants and intermediate levels of CF, the concentration of electrolytes is 40-60 mmol/L. A concentration of less than 40 mmol/L in an individual indicates absence of disease. However, a few patients of CF have reported normal ion levels in the sweat.^[11] A consultation of family history is recommended in such cases. Currently, cystic fibrosis is being diagnosed through biosensors, which detect and measure the levels of chloride ions.

2.3.1 Chloridometer (Titration)

A chloridometer is a device in which the principle of coulometric titration is used for the measurement of chloride ion concentration in a solution. ChloroCheck Chloridometer is one such example. For the diagnosis of CF, a 10 ul of sweat sample is added to the acid buffer solution, acting as a stabilizer. Subsequently, silver ions are generated through electrolysis of silver electrodes and these silver ions combine with the chloride ions in the sample. Therefore, the chloride ions are quantified through the electric current and silver ions.^[12]

2.3.2 Chromogenic Anion Sensors

The chromogenic anion sensor, tungsten oxide is exploited for its electrochromic properties. The levels of sodium chloride are measured in the sample through this device. 3 ul of sweat serve as our sample. Upon the interaction with sodium ions, an oxide blue concentration occurs whose intensity corresponds to the number of ions. It was deduced from the results that the sensor displays productive transmittance modulation. At 555nm, solutions of sodium ions at different concentrations showed different transmittance modulations; 48% for 120 mmol/l, 35% for 90 mmol/l, 15% for 60 mmol/l, and 7% for 30 mmol/l. Therefore, the device qualifies as a colorimetric test for CF. Despite the above-mentioned favourable results, chromogenic sensors are unable to distinguish between different anions.^[13]

2.3.3 FRET Flow Cytometry

Neutrophil Elastase (NE), a serine protease can be used as an indicator of CF. It originates in the neutrophils. A decline in lung function due to CF is indicated by the presence and enhanced action of NE.^[14] The quantification of NE activity and its further analysis for the detection of CF can be performed through flow cytometry, Forster Resonance Energy Transfer (FRET) probe and FRET-based reporter NEmo-2E. Although, confocal microscopy also helps in the observation of NE activity, an improved signal/noise ratios were observed in FRET flow cytometry using NEmo-2E reporter which is also a faster, more efficient and a simpler technique.^[15] However, the assays used in FRET Flow Cytometry are relatively expensive and require expert handling.

2.3.4 Electrochemical Chloride Quantification

Screen-printed electrochemical sensors can be used for timely diagnosis of CF. The quantification of chloride ions in the sweat sample is achieved through such devices. A pHEMA membrane containing potassium chloride is used as a reference electrode for this purpose. A 6.3 ± 0.9 mV drift was shown by the electrodes with the chloride ions in the 10-100mmol/l range.^[16]

However, the conductive materials used in electrochemical biosensors give rise to concerns regarding their safety as they can cause irritation and allergies upon contact to the skin. This problem can be solved by using water-based electrochemical biosensors, but an ionic surfactant is required to disperse the conductive materials. It results in the decrease of conductance due to the hindrance caused by the surfactant. Furthermore, an increase in cost occurs due to the use of ionic surfactants.^[17]

2.4 Use of Nanotechnology in Diagnostics

Nanotechnology is an interdisciplinary field integrating medicine, biology, chemistry, and engineering. A great diversity of nanoparticles has been synthesized during the last few decades and are being increasingly tested for their diagnostic and therapeutic potential.

However, not all nanoparticles are synthetic. A variety of particles extracted from sulphur, soot, inorganic ash, and the others present in wells and air are all derived from nature. Moreover, bacteria and yeast also produce nanoparticles of sulphur and selenium. Scientists are showing an increased interest in the exploration and extraction of natural nanoparticles in the developing fields of phyco and phyto-nanotechnology. (Sharoon Griffin et al)^[18] There is a wide range of application of synthetic nanoparticles which are found as nanocomposites (adsorbed to a solid body), powder, fluids, gases etc. This category also includes liposomes, micelles, and vesicles. ^[19]

Nanotools are being developed for their application in disease diagnostics which include nanowires, liposomes, dendrimers, cantilevers etc. for the detection of various biomarkers in oncology and quantum dots for cancer research and imaging. (Dr. Hamed Laroui et al).^[20]

In our study, we exploited these diagnostic properties of nanoparticles in our quest to determine the diagnostic potential to silica nanoparticles for the diagnosis of CF by measuring the level of chloride ions in sweat sample.

2.5 Silica Nanoparticles (SiO₂)

Silica nanoparticles, which are also known as silica dioxide or nano-silica, is currently the centre of research for biomedical sciences due to the extraordinary properties it possesses that include biocompatibility, bio-sensing and even bio-imaging. They are further divided into a number of types based on their pore rate, size differences, conductivity, polymeric nature, specific properties attained due to the coating material and morphology, etc. Following are some of the general characteristics of silica nanoparticles.

2.5.1 Physicochemical properties

Silica nanoparticle appears to be in the form of dry white powder and are hygroscopic in nature.^[21] They usually appear to have a spherical smooth shape, and the nano size of particles provides them a higher specific surface area as compared to the outdated methods. The larger surface-to-volume ratio along with the reflective properties of modified silica nanoparticles is the reason behind the numerous applications of nano-silica in our daily lives.^[22]

Elements	Chemical Composition
Oxygen	53.33%
Silicon	46.83%

Table 3 Chemical composition of Silica

It has been observed that density, optical properties as well as the physicochemical properties demonstrate changes if the size of silica nanoparticles are altered. The decrease in size of silica nanoparticles also causes an increase in the intensity of blue and green bands due to increased silanol concentration

Properties	Metric
Density	2.4 g/cm ³
Molar Mass	59.96 g/mol
Melting point	1600 °C
Boiling point	2230 °C

Table 4 Physicochemical Properties of silica

2.5.2 Drug delivery through SiNPs

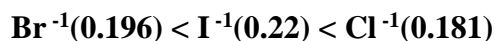
Silica nanoparticles are used to deliver the drug molecule as well as DNA molecules accurately to the target site. Since the DNA molecule and the silica nanoparticles are negatively charged, they need to be modified by adding functional group or silylation to bind the DNA molecule to its surface.^[23] Once the mesoporous silica nanoparticle is formed the DNA binds to it easily and can be delivered to the exact target.

Drug molecules are also attached to the mesoporous silica nanoparticles due to the diverse pore size of the nano silica. But to caps the drug molecule with silica nanoparticle, gold nanoparticles are used. Once these modified drugs carrying silica nanoparticles reach the site, the covalent bond is broken with the help of certain molecules. This allows the pore to open and deliver the drug to its target site.

2.5.3 Adsorption

One of the many fascinating properties of silica nanoparticles is its ability to adsorb metals and ions to its surface. This property acts as a cue for scientists to detect and measure the number of salts present in a body. It has also been observed that the enhanced clusterisation of water at a mesoporous silica nanoparticle. The enhanced clusterisation of water molecules causes a reduction in the solvent activity that results in an increase in the adsorption ability of nano silica.

The reduced desolvation energy causes the adsorption of anions to the modified surface of silica nanoparticles. Upon comparison among the anions, it was observed that the chloride ions tend to be adsorbed more to the silylated silica nanoparticles than to simple silica nanoparticles. The efficiency in adsorption of anions is demonstrated below



I.F. Mironyuk et al. deduced after carrying out a set of experiments that silylation silica nanoparticles adsorbed 1.34 mmol/g of Cl^{-1} from 0.01M CaCl_2 . Thus, indicating that the adsorption capacity of silylated silica nanoparticles increases up to eight times in comparison to the adsorption carried out by unmodified silica nanoparticles.^[24] This characteristic of silica nanoparticle offers us the exceptional opportunity to detect small amount of salt changes in our body. Thus, playing a vital role in the diagnosis of cystic fibrosis which is one

In short, it has been observed that the interaction between the silica nanoparticles and ions indicate a salt independent Van der Waal attraction mechanism which is the increasing osmotic pressure of ions in the solution that compete with the elevating salt concentration and ion solvation. Therefore, surface tension is known to create the difference between silica and different salts.^[25]

2.6 Rationale

Diagnostic techniques already being used for CF are expensive and can be considered unsafe in case of electrochemical biosensors. For the conventional sweat test, a larger amount of sweat is required which might be inconvenient for the patient. Due to the lack of time-efficient and cost-effective diagnosis techniques for CF, there is a requirement of sensitive and cheap tools to make its diagnosis easier. The cost-effectiveness, easier synthesis, adsorptive properties, and low detection limit of SiNPs lead to the investigation for their role as potential diagnostic agents in the measurement of chloride ion concentration for the diagnosis of CF.

2.7 Aims and Objectives

There are four main objectives of this study:

- 1) To obtain protein models for the visualization of wild-type and mutant CFTR
- 2) To study the docking of CFTR with drugs to observe their interactions
- 3) To extract silica nanoparticles from Karakoram clay
- 4) To quantify chloride ions adsorbed on SiNPs

Chapter 3

Materials and Methods

3 Materials and Methods

3.1 Software and programs

Swiss-Model was used for protein modelling to obtain 3D structure. *DoGSiteScorer: Binding Site Detection on ProteinsPlus* was used to determine the pocket in the protein and determine its coordinates for the grid box in docking. Initially, PyRx Virtual Screening Tool but mainly *UCSF Chimera* was used for the procedure of docking the ligand and protein through a local extension of *AutoDock Vina*. *UCSF Chimera* was also used, initially, for visualization and modifications of protein and ligand structures. *PyMol* was mainly employed for visualization and display of protein and ligand interactions. *PLIP Web Tool* was used mainly for visualizing the binding sites and bonds formed between protein-ligand interactions.

3.2 Preparation of ligand structures for Ivacaftor, Elexacaftor and Tezacaftor

Three drugs, Ivacaftor, Elexacaftor and Tezacaftor, were used as ligands against the protein. The ligands were downloaded in SDF file format from PubChem Compound Database, that were converted to PDB file format in *UCSF Chimera*. The ligand structures in PDB format were converted to PDBQT format using the local extension of *AutoDock Vina* in *UCSF Chimera* to prepare it for docking.

3.3 Preparation of protein structure for Cystic Fibrosis Transmembrane Conductance Regulator (CFTR)

The 3D structure of the wildtype CFTR protein was downloaded from the RCSB protein data bank that was encoded with the PDB ID 6MSM. The 6MSM structure is phosphorylated, ATP-bound CFTR. The PDB format was also converted to the PDBQT file using the local extension of *AutoDock Vina* in *UCSF Chimera* when prepare it for docking.

For the drug interaction with the mutation of interest in CFTR protein, the FASTA sequence of the 6MSM was edited at the 95th position where lysine was replaced with glutamine. This edited FASTA sequence was uploaded to the *Swiss-Model* to obtain and download the PDB format of a 3D structure of a CFTR protein with the K95Q mutation. The structure modelled had 99.93% sequence identity with the wildtype 6MSM CFTR.

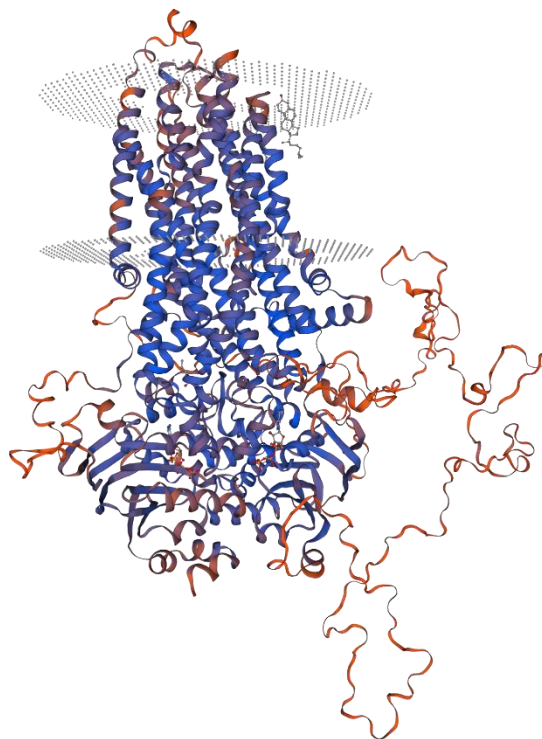


Figure 5: Mutant 6MSM CFTR with K95Q mutation

3.4 Docking Protocol

Molecular docking was executed by using *Autodock Vina* in *UCSF Chimera*. Each of the three ligands were docked with the wildtype and the mutant protein, respectively. Therefore, the PDB files of a ligand and a protein type were opened in *UCSF Chimera* for each proteindrug interaction. As the interactions same grid coordinates (grid center) and grid boxes were the same for all the runs. The said pocket was selected due its proximity to the amino acid under observation. The grid coordinates and radius were obtained from *DoGSiteScorer*. The grid size was set at the given maximum radius of 17.28x17.28x17.28 (x,y,z) points and the grid center was sized at 153.89, 153.57, 176.03 at x, y and z dimensions respectively, in *AutoDock Vina*.

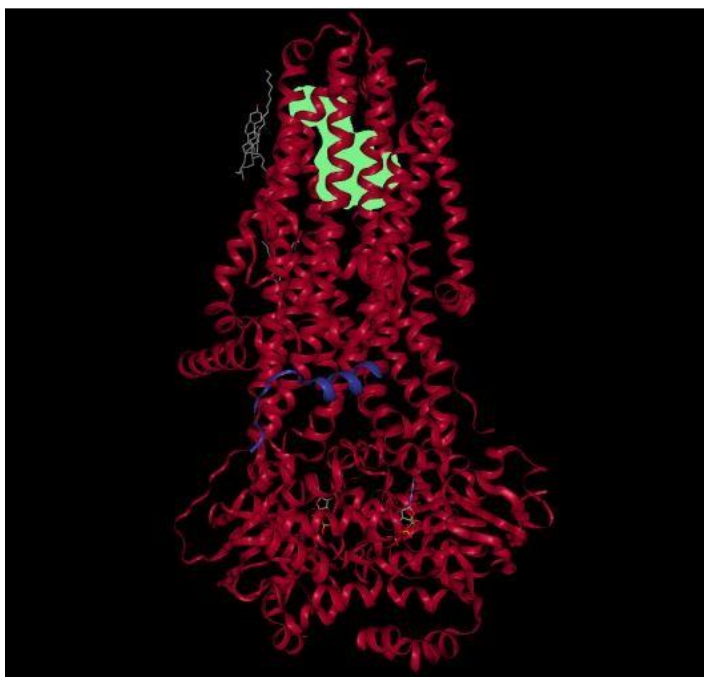


Figure 7: 6MSM CFTR with a highlighted pocket

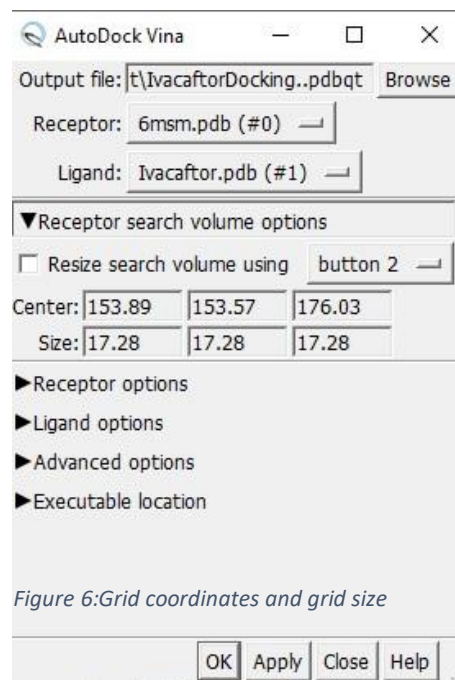


Figure 6: Grid coordinates and grid size

An output source was browsed prior the docking so that the prepared file in PDBQT format would be saved in it. The ligand was docked to the active sites of the pocket in the protein. Their binding affinities (ΔG values), lower and higher RMSD values were saved. After docking, the PDBQT files were visualized in PyMol.

3.5 Post-Docking analyses

The PDBQT files of the post-docking drug and protein are visualized in *PyMol* where each binding mode is separated and viewed individually. Each binding mode with the protein is saved in PDB format.

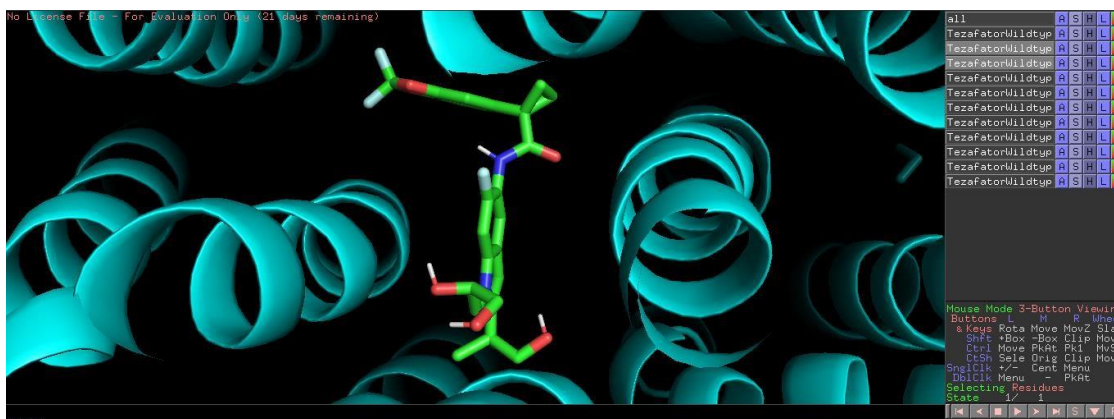


Figure 8: Visualization of protein-ligand interaction in PyMol

Subsequently, the PDB file is uploaded to PLIP Web Tool to view the binding interactions the drug with the binding sites of the protein pocket.

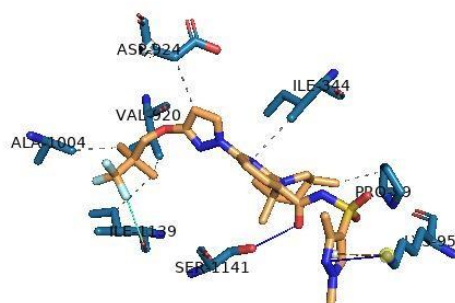


Figure 9: Intermolecular interactions in PLIP

3.6 Synthesis of Silica Nanoparticles (SiNPs)

To synthesis silica nanoparticles, a top-down approach was used in which the silica nanoparticles were created from scratch from the clay extracted from the Karakorum mountains. A set of instruments and chemicals were also used during this process that are listed below.

Chemicals	Equipment
□ Ethanol (C ₂ H ₆ O)	□ Flasks, beaker
□ Hydrochloric Acid (HCl, 36% concentrated)	□ Magnetic stirrer

<input type="checkbox"/> Nitric Acid (HNO_3 , concentrated)	65%	<input type="checkbox"/> Hot magnetic stirring plate
<input type="checkbox"/> Sodium Hydroxide (NaOH)		<input type="checkbox"/> Thermometer
<input type="checkbox"/> Bentonite Clay		<input type="checkbox"/> Clamp stand
		<input type="checkbox"/> Pipettes and tips
		<input type="checkbox"/> Centrifuge
		<input type="checkbox"/> Concentrator
		<input type="checkbox"/> Forceps, Falcons
		<input type="checkbox"/> Funnel
		<input type="checkbox"/> Filter paper
		<input type="checkbox"/> pH paper

Table 5: Chemicals and Equipment

Bentonite clay, extracted from the Karakorum mountains, was first of all sieved through a small mesh of size up to 100 μm . This assisted in removing any impurities from the clay in the beginning to avoid contamination of silica nanoparticles. Then the clay was placed carefully inside a muffle furnace at an extremely hot temperature at 680 $^{\circ}\text{C}$ for a time period of about one hour only.



Figure 10: Clay placed in muffle furnace

After that the clay was accurately measured up to 100 g and dissolved in a 1000ml of 2.5M of HCl. The solution was placed on a hot magnetic stirring plate in at 90°C for two hours. Then the solution was filtered to separate the residues of bentonite rich clay. The acidic bentonite rich clay residues were repeatedly washed with water and the pH paper was used to evaluate the neutralization level.



Figure 11: Clay dissolving in HCl



Figure 12: NaOH treated clay being filtered

A 10wt% sodium silicate solution (SSS) was then prepared by mixing the bentonite rich clay in 2M of NaOH solution. The flask was containing the SSS was then placed on an oil bath at 90°C for 2 hours again. Later on, the solution was removed from the oil bath and filter to remove any unwanted residues from the SSS.

To neutralize the alkaline SSS solution, a solution of 5M of HNO₃ was prepared along with 10 ml of ethanol which acts as a co-solvent. The acidic solution was slowly added to the alkaline SSS and continuously measured with pH paper to achieve neutralization. The neutralized solution was then placed in centrifuge for about 10 minutes at 6000 rpm room temperature. After the centrifugation of the solution a prominent pallet was obtained which consists of our silica nanoparticles. [26]

3.7 Characterization

The silica nanoparticles prepared from Karakoram mountains were further characterized using Scanning Electron Microscopy (SEM) and Fourier – Transform Infra-Red Spectrometry (FTIR).

3.7.1 Scanning Electron Microscopy (SEM)

The clay extracted from the Karakoram mountains were further washed repeatedly to remove any impurities present in the white pallet of silica nanoparticles. Then a very small amount of silica nanoparticles was added in ethanol taken in a falcon. All these solutions were probe ultrasonicated 60 kHz for 30 seconds to remove any aggregates in the solutions. The solution was repeatedly sonicated properly for SEM and placed on ice to make sure that the solution remains chill.

A diamond cutter is used for cutting proper slides for SEM, which need to be treated with ethanol to remove any impurities. Then using a pipette, a small drop is placed on the slide in such a manner that the sample is placed in the center of the slide. You should make sure that

you place a small drop to avoid any overflow. Do not touch the slide and leave it dry for some minutes as the ethanol evaporates quickly allowing the sample to be fixated [27]

After the sample has been fixated, it is mounted on a holder typically metallic in nature such as aluminium with the help of double sticky tape. This holds the sample in place and coating the sample with platinum, gold and silver ensures proper imaging of the sample.

3.7.2 Fourier-Transform Infra-red Spectroscopy

While scanning electron microscopy (SEM) directs electron beam on a small amount of silica nanoparticle pallet homogenized in ethanol to detect its morphology, Fourier-transform infrared (FTIR) spectroscopy uses infra-red wavelengths and yields frequency differential bands corresponding to specific functional bond stretching interactions of our sample.

The slide used in FTIR was prepared using potassium bromide and was then placed under pressure for few minutes.^[28] The sample was then uploaded on the newly prepared slide and inserted into the machinery. The sample absorbs the infrared light at different frequencies which indicates the chemical bonds present in the sample.

3.8 Adsorption of chloride ions

To calculate the amount of chloride ions adsorbed on silica nanoparticles, a 0.166M of silica nanoparticle solution was prepared. And a 0.12M of NaCl solution was taken as a source of chloride ions. A solution was prepared of 1 ml of silica nanoparticles and 5 ml of sodium chloride. The solution was then placed on a magnetic stirring plate for 4 hours.

Mohr's method of titration was used to calculate the chloride ion concentration present in solution of nano silica and sodium chloride. A 0.1M of silver nitrate (AgNO_3) solution was prepared to be used as a titrant and 0.25M of potassium chromate (K_2CrO_4) solution was used as an indicator. Few drops of K_2CrO_4 solution were added in the nano silica and sodium chloride solution, which causes the solution to appear as yellow. The AgNO_3 solution is titrated against this yellow solution at a slow speed.

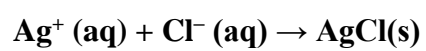


Figure 13: Titration

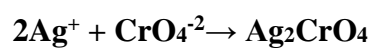


Figure 14: white precipitates

Gradually, white precipitates start to appear in solution, this indicates the formation of AgCl salt. The reaction occurring during this time period is mentioned as following.



The excessive silver ions present in solution then react with the chromate ions to form silver chromate, from our indicator K_2CrO_4 solution. This reaction is demonstrated as below and can be indicated by the formation of reddish brown colour.



Chapter 4

Results and Discussions

4 Results and Discussions

4.1 Docking

Docking simulations of the three drug ligands with the wildtype and mutant 6MSM CFTR protein were run that showed their binding affinities (ΔG values) in kcal/mol.

4.1.1 Wild-type protein-drug interaction

In the wildtype protein-ligand interactions, ivacaftor had the ΔG value -7.2 kcal/mol at its 1st conformation or lowest conformation, whereas elexacaftor and tezacaftor had ΔG value, -8.0 kcal/mol and -8.4 kcal/mol, respectively. As the ΔG value at the lowest conformation is most stable,^[29] the results indicates that, out of the three drug ligands, tezacaftor possess the greatest binding affinity for the wildtype CFTR.

Ligand (Drug)	Lowest (1st) to highest (9th) conformation binding affinities in ΔG (kcal/mol)								
	1st	2nd	3rd	4th	5th	6th	7th	8th	9th
Ivacaftor	-7.2	-6.5	-6.5	-6.5	-6.5	-6.3	-6.2	-6.2	-6.0
Elexacaftor	-8.0	-7.1	-6.6	-6.5	-6.5	-6.1	-6.1	-6.0	-6.0
Tezacaftor	-8.4	-8.3	-8.1	-7.8	-6.9	-6.0	-6.0	-6.0	-5.9

Table 6: Binding affinities of ivacaftor, elexacaftor and tezacaftor at the binding sites of wildtype CFTR pocket.

4.1.2 Mutant protein-drug interaction

To observe interaction of the same three drug compounds but in a mutant CFTR with a specific amino acid (Lys95) substituted (Glu), the binding affinities were different when recorded. The ΔG value of ivacaftor, elexacaftor and tezacaftor were shown to be -7.9 kcal/mol, -8.2 kcal/mol, -7.9kcal/mol, respectively. In the mutant protein-drug interaction, elexacaftor was shown to have the greatest affinity to CFTR.

Ligand (Drug)	Lowest (1st) to highest (9th) conformation binding affinities in ΔG (kcal/mol)								
	1st	2nd	3rd	4th	5th	6th	7th	8th	9th
Ivacaftor	-7.9	-7.3	-6.9	-6.6	-6.5	-6.1	-6.1	-5.6	-5.5
Elexacaftor	-8.2	-6.9	-6.5	-6.2	-6.2	-5.9	-5.6	-5.5	-5.3
Tezacaftor	-7.9	-7.8	-7.7	-7.6	-6.7	-6.4	-6.0	-6.0	-6.0

Table 7: Binding affinities of ivacaftor, elexacaftor and tezacaftor at the binding sites of mutant CFTR pocket.

When a ligand binds to a protein, it brings in a conformational change. This change occurs through the intermolecular interactions for instance, hydrogen bonding, electrostatic forces, hydrophobic interactions etc. These ligand-receptor interaction is a requirement for signal transduction,^[30] which creates a theoretical foundation for new drug discovery and development. The strength of these interactions or binding affinities are somewhat indicative of the protein-ligand complex stability and can be a steppingstone for further studies.

To compare the data shown in Table 6 and 7, the binding affinities of ivacaftor and elexacaftor becomes smaller during its interaction with the mutant (K95Q) protein which may suggests that the intermolecular interactions are increased either in number or in strength or in both. which on further analysis, may indicate that their much stronger affinity, as compared to those shown in the wildtype protein, likely be due to the mutation (K95Q) present in the protein. On the other hand, tezacaftor's binding affinity increases in the mutant protein, which indicates stronger interaction to the wildtype protein. The ΔG values provides information about the ligand docking at the active site in the protein pocket, but it may also suggest ligand binding in a suitable conformation.^[31] However, the current docking techniques employed does not definitively describe the protein-ligand interaction and accurately relate it to the docking affinities.^[32] Therefore, this computational data of binding affinities does not prove or confirm these interactions without the in vitro experiments supporting these findings.

4.2 Post-docking Analysis

In subsequent analysis, the post-docking files were visualized through PLIP Web Tool to analyze the types of interaction of the drugs with the wildtype and protein in general and the specific mutation (K95Q) in particular.

Ivacaftor forms five hydrophobic interactions with the wildtype CFTR including Lys95, Phe337, Ile340, Val920, Asn1138 and three hydrogen bonds including Arg134, Ser341, Ser1141. The intermolecular interactions of Elexacaftor are mainly hydrophobic interactions.

These eight are: Pro99, Ile344, Val920, Asp924, Ala1004, Ile1139 and two hydrogen bonds, Lys95, Ser1141. Tezacaftor forms six hydrophobic interactions: Lys95, Ile344, Ile344, Val345, Asp924, Thr1142 and six hydrogen bonds: Arg134, Arg347, Asn1138, Ser1141, Ser1141, Gln1144.

Ligands (Drug)	Lowest Binding Affinity (kcal/mol)	Amino acids involved in wildtype CFTR	
		Hydrophobic Interactions	Hydrogen Bonding
Ivacaftor	-7.2	Lys95, Phe337, Ile340 Val920, Asn1138	Arg134, Ser341, Ser1141
Elexacaftor	-8.0	Pro99, Ile344, Val920, Asp924, Ala1004, Ile1139	Lys95, Ser1141
Tezacaftor	-8.4	Lys95, Ile344, Ile344, Val345, Asp924, Thr1142	Arg134, Arg347, Asn1138, Ser1141, Ser1141, Gln1144

Table 8: Interactions of ivacaftor, elexacaftor and tezacaftor at the binding sites of wildtype CFTR pocket.

The molecular interactions that Ivacaftor forms are five hydrophobic interactions with the mutant CFTR including the mutant Glu95, Phe337, Val345, Val920, Asn1138 and three hydrogen bonds including Arg134, Ser341, Ser1141. The intermolecular interactions of Elexacaftor are mainly hydrophobic interactions. These nine are: Pro99, Ile344, Val920,

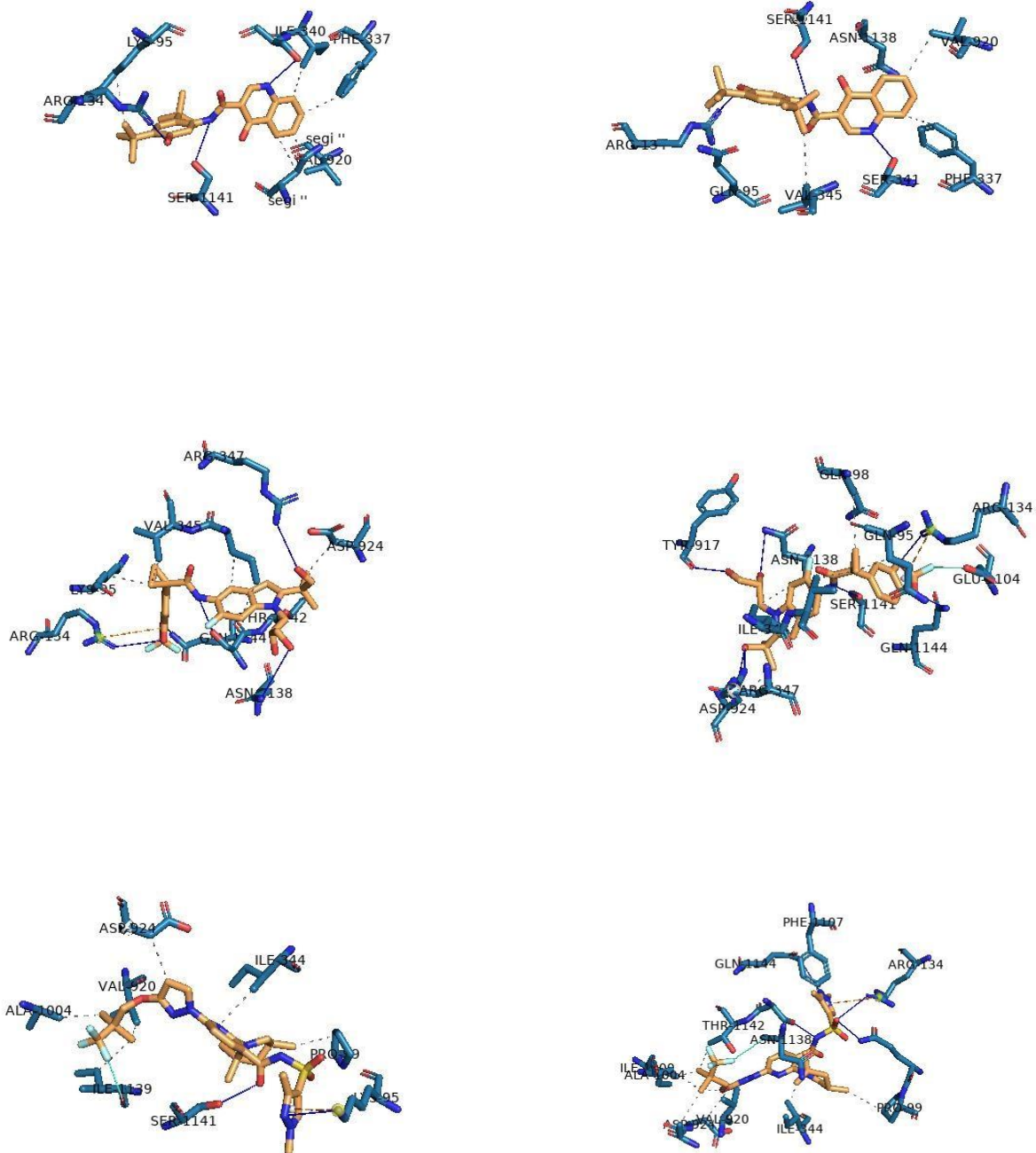
Ala923, Asp924, Ile1000, Ala1004, Phe1107, Thr1142 and five hydrogen bonds, Gln98, Arg134, Ser1141, Ser1141, Gln1144. Tezacaftor forms six hydrophobic interactions: Gln95, Gln98, Ile344, Ile344, Val345, Asp924 and eight hydrogen bonds: Arg134, Arg347, Tyr917, Asp924, Asn1138, Ser1141, Ser1141, Gln1144.

Ligands (Drug)	Lowest Binding Affinity (kcal/mol)	Amino acids involved in mutant CFTR	
		Hydrophobic Interactions	Hydrogen Bonding
Ivacaftor	-7.9	Gln95, Phe337, Val345, Val920, Asn1138	Arg134, Ser341, Ser1141
Elexacaftor	-8.2	Pro99, Ile344, Val920, Ala923, Asp924, Ile1000, Ala1004, Phe1107, Thr1142	Gln98, Arg134, Ser1141, Ser1141, Gln1144
Tezacaftor	-7.9	Gln95, Gln98, Ile344, Ile344, Val345, Asp924	Arg134, Arg347, Tyr917, Asp924, Asn1138, Ser1141, Ser1141, Gln1144

Table 9: Interactions of ivacaftor, elexacaftor and tezacaftor at the binding sites of wildtype CFTR pocket.

The three drugs in the wildtype CFTR all bind to the amino acid Lys95 with ivacaftor and tezacaftor through hydrophobic interaction while elexacaftor through hydrogen bonding. But in the mutant CFTR, when the lysine is replaced by glutamine at 95th position, elexacaftor does not bind to it at all. Ivacaftor and tezacaftor does bind through hydrophobic interaction to the glutamine. While Ivacaftor binding affinity decreases in the mutant CFTR, the tezacaftor's increases. This is suggestive that Ivacaftor is likely to be the suitable drug of the three drugs to treat the K95Q mutation. Even more so, hydrophobic interactions contribute more to protein

stability than hydrogen bonding, which may be a stronger force but maintaining folding and stability is increased more with hydrophobic interactions.[5] Ivacaftor is FDA-approved for R117H mutation [6] among 23 others, which is a class IV mutation. Therefore, K95Q, which is also a Class IV mutation, can likely be said to be treated by ivacaftor. Potentiators such as ivacaftor can help open the CFTR channel, and also help increase the function of normal CFTR.



4.3 Synthesis of Silica nanoparticles

After the above-mentioned extraction method of silica nanoparticles from clay, the following pellet was obtained.



Figure 16: Silica nanoparticles' pellet

4.4 Characterisation

The results obtained after SEM and FTIR are shown below

4.4.1 SEM

The following SEM images show that the size of our SiNPs was 80 ± 40 nm and they were circular in shape

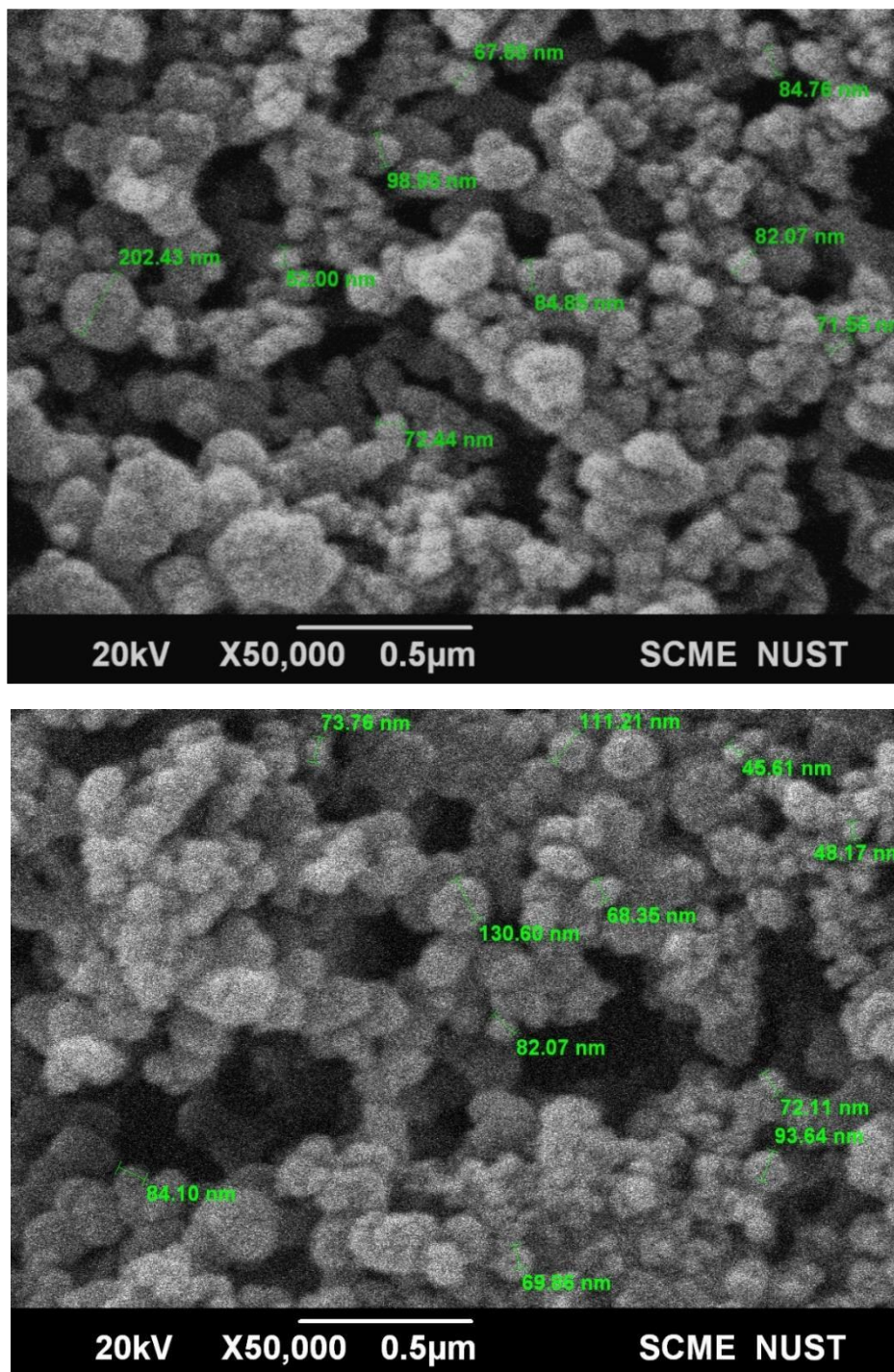


Figure 17: SEM images with measurements

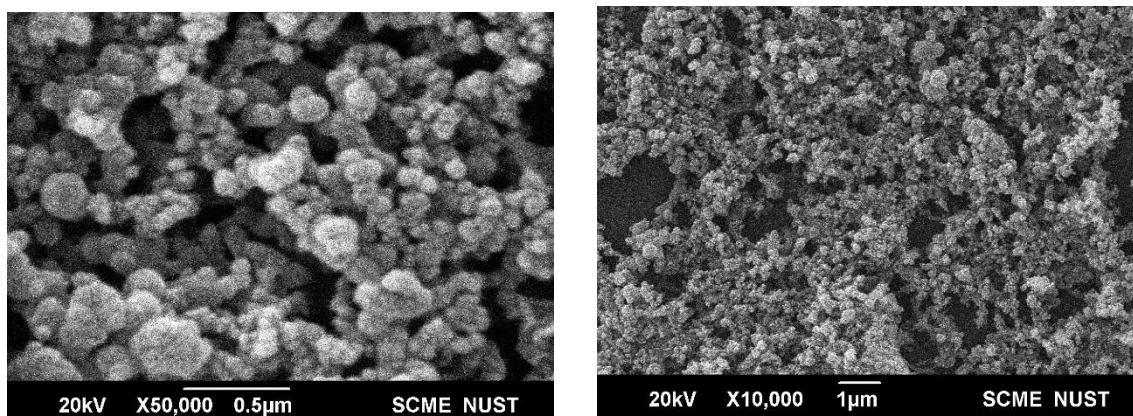


Figure 18: SEM images of SiNPs

4.4.2 FTIR Spectrum

FTIR uses infra-red wavelengths and yields frequency differential bands corresponding to specific functional bond stretching interactions of our sample. The spectrum obtained in FTIR spectroscopy confirms the characteristics bond stretching which corresponds to SiNPs.(12)

The peaks below 1500cm^{-1} are called fingerprints. It is only used in cases where we have very similar compounds. Different functional groups can give the peaks in the same region of the spectrum. However, they are distinguished by different features of peaks. For instance, based on intensity, peaks can be weak, medium, or strong. Some peaks in the spectrum are broad while others are sharp.

The Si-O-Si symmetric stretching, Si-OH stretching, and Si-O-Si asymmetric stretching vibrations were indicated by the peaks at 721cm^{-1} , 1046cm^{-1} and 1085cm^{-1} frequency, respectively. The O-H bending vibration mode of physisorbed water molecules caused the peak at 1635cm^{-1} . The broad peak at 3421cm^{-1} is formed due to the stretching vibration of the hydrogen-bonded Si-OH and hydroxyl of physisorbed water molecules.^[33]

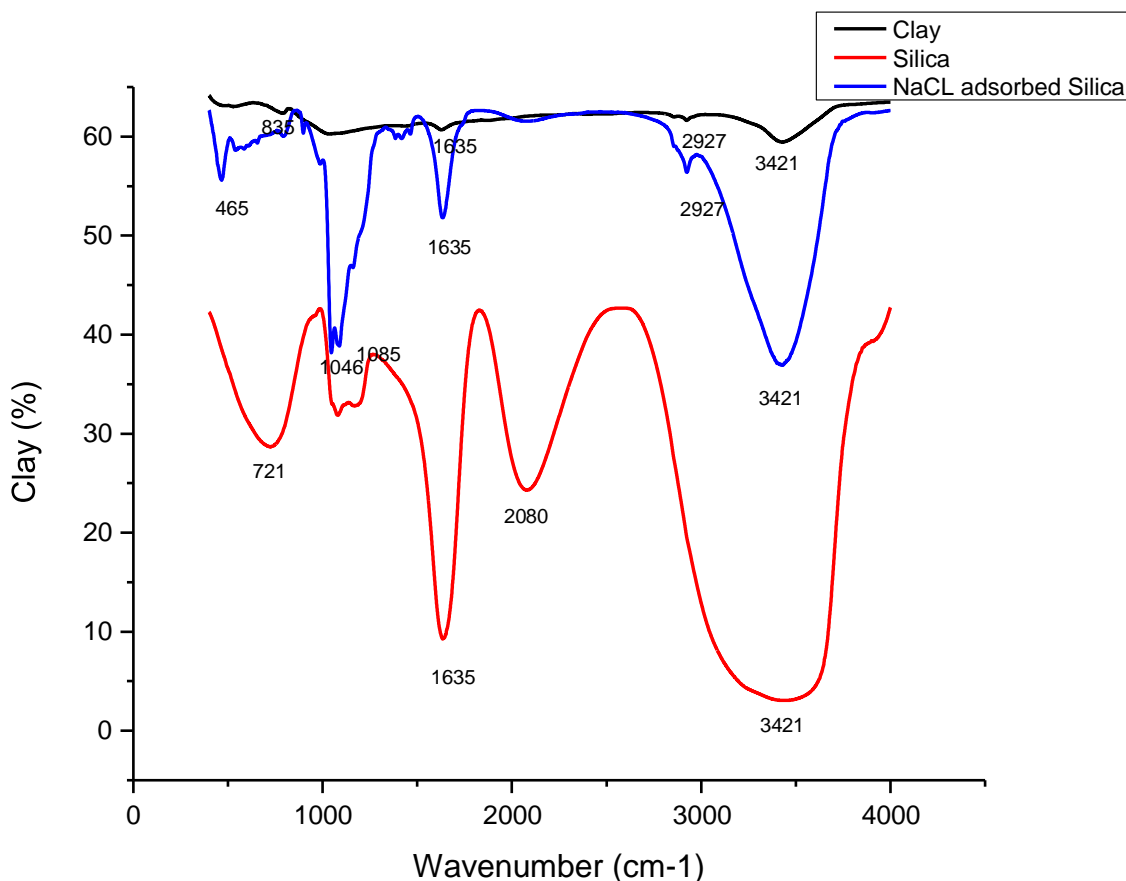


Figure 19: FTIR spectrum

For the sake of comparison, we performed FTIR analysis of Karakoram clay, SiNPs and SiNPs which had Cl^{-1} ions adsorbed to them. The difference in peaks indicates a change in composition of clay when SiNPs are extracted from it and further different peaks after the adsorption of Cl^{-1} confirm the adsorption and that the Cl^{-1} caused a change in silica nanoparticles' composition.

4.5 Adsorption

By using the following formula, we determined the chloride ion concentration of our supernatant samples which was then subtracted from our original molarity of NaCl solution.

$$\text{Cl}^{-1} \text{ concentration} = (A * N * 34.45) / V$$

Where,

A = Volume of Ag NO_3 titrated

N= Normality of Ag NO₃

V= Volume of sample used

The following data was obtained. Triplicates were performed to improve accuracy.

Serial Number	Volume of titrant(ml)	Cl ⁻¹ concentration(g/L)	Molarity of Cl ⁻¹ in supernatant(M)	Cl ⁻¹ adsorbed to silica(M)
1)	1.1	0.73	0.021	0.099
2	1.5	0.886	0.025	0.095
3)	1.3	0.768	0.022	0.098

Table 10: Cl⁻¹ calculated after titration

Volume of titrant was determined at the following point of titration



Figure 20: End point of titration

Chapter 5

Conclusion and Future prospects

Conclusion and Future prospects

The promising results we obtained from our *in silico* and *in vitro* research project demonstrates the diagnostic potential ability of silica nanoparticle to detect minute alteration in chloride ion concentration accurately present in the sweat of Cystic Fibrosis patients. With further advancement in research, we will be successful enough to develop a diagnostic kit that will not only be accessible but require less sweat concentration requirements.

Furthermore, we are confident that in the future with advanced research silica nanoparticles will be used in the delivery of drugs to specific mutative sites not only for Cystic Fibrosis but other diseases too. The nano-size and the stable configuration of silica nanoparticles is the reason behind such progressive research. But there are some hurdles such as the side effects and the increase in the cytotoxic effect of silica nanoparticles if they are used in excess, We are optimistic that with a suitable combination of other materials all such hurdles can be conquered in research as well as healthcare facilities.

References

- [1] P. B. Davis, "Cystic Fibrosis Since 1938," *American Journal of Respiratory and Critical Care Medicine*, pp. 173(5):475-82, 2006.
- [2] Linsdell, P., 2006. Mechanism of chloride permeation in the cystic fibrosis transmembrane conductance regulator chloride channel. *Experimental physiology*, 91(1), pp.123-129
- [3] Lopes-Pacheco, M., 2016. CFTR modulators: shedding light on precision medicine for cystic fibrosis. *Frontiers in pharmacology*, 7, p.275.
- [4] Ge N, Muise CN, Gong X & Linsdell P (2004). Direct comparison of the functional roles played by different membrane spanning regions in the cystic fibrosis transmembrane conductance regulator chloride channel pore. *J Biol Chem* 279, 55283–55289.
- [5] Bergaya, F.; Lagaly, G. (2006). "Chapter 1 General Introduction: Clays, Clay Minerals, and Clay Science". *Developments in Clay Science*. 1: 1–18.
- [6] Gong X & Linsdell P (2003c). Mutation-induced blocker permeability and multiion block of the CFTR chloride channel pore. *J General Physiol* 122, 673–687.
- [7] Tsui LC. The spectrum of cystic fibrosis mutations. *TIG* 1992; 8:392–398.
- [8] Sheppard DN, Rich DP, Ostedgaard LS, Gregory RJ, Smith AE, Welsh MJ. Mutations in CFTR associated with mild-disease form Cl channels with altered pore properties. *Nature* 1993; 362:160–164
- [9] Kerem E, Kerem B. Genotype-phenotype correlations in cystic fibrosis. *Pediatr Pulmonol* 1996;22:387–395.
- [10] Kerem E, Rave-Harel N, Augarten A, Madgar I, Nissim-Rafinia M, Yahav Y, Goshen R, Bentur L, Rivlin J, Aviram M, Genem A, Chiba-Falek O, Kraemer MR, Simon A, Branski D, Kerem B. A cystic fibrosis transmembrane conductance regulator splice variant with partial penetrance associated with variable cystic fibrosis presentations. *Am J Respir Crit Care Med* 1997;155: 1914–1920.

-
- [11] Welsh MJ, Smith AE. Molecular mechanisms of CFTR chloride channel dysfunction in cystic fibrosis. *Cell* 1993;73:1251–1254
- [12] B. J. Rosenstein and G. R. Cutting, "The Diagnosis of Cystic Fibrosis: A Consensus Statement. Cystic Fibrosis Foundation Consensus Panel," *The Journal of Pediatrics*, pp. 132(4):589-95, 1998.
- [13] Zhang, C., Kim, J., Creer, M., Yang, J. and Liu, Z., 2017. A smartphone-based chloridometer for point-of-care diagnostics of cystic fibrosis. *Biosensors and Bioelectronics*, 97, pp.164-168.
- [14] V. D. Matteis, A. Cannavale, L. Blasi, A. Quarta and G. Gigli, "Chromogenic device for Cystic Fibrosis precocious diagnosis: A "point of care" tool for sweat test," *Sensors and Actuators B Chemical*, p. 225, 2015.
- [15] A. S. Dittrich, I. Kühbandner, S. Gehrig, V. Rickert-Zacharias, M. Twigg, S. Wege, C. C. Taggart, F. Herth and C. Schultz, "Elastase Activity on Sputum Neutrophils Correlates With Severity of Lung Disease in Cystic Fibrosis," *The European Respiratory Journal*, p. 51(3):1701910, 2018.
- [16] D. Frey, A. Dittrich, I. Kuhbandner, A. Halabatyi, M. Hagner, M. Guerra, S. Wege, V. Halls, F. Herth, C. Schultz and M. Mall, "Small-molecule FRET flow cytometry: a novel technique to monitor surface-associated protease activity in cystic fibrosis," *Journal of Cystic Fibrosis*, pp. Volume 18, Supplement 1, S119. Page 219, 2019.
- [17] J. Gonzalo-Ruiz, R. Mas, C. Haro, E. Cabrujaa, R. Camero, M. A. Alonso-Lomillo and F. J. Muñoz, "Early determination of cystic fibrosis by electrochemical chloride quantification in sweat," *Biosensors and Bioelectronics*, pp. Volume 24, Issue 6, Pages 1788-1791, 2009.
- [18] R. P. Tortorich, H. Shamkhalichenar and J.-W. Choi, "Inkjet-Printed and Paper-Based Electrochemical Se
- [19] Griffin S, Masood MI, Nasim MJ, et al. Natural Nanoparticles: A Particular Matter Inspired by Nature. *Antioxidants (Basel)*. 2017;7(1):3. Published 2017 Dec 29. doi:10.3390/antiox7010003
- [20] (Christina Raab et al) Nanopartikel-Materialien der Zukunft, Albert Rössler, Georgios Skillas, Sotiris E. Pratsinis; *Chemie in unserer Zeit*, 2001, 1, 32-41.

-
- [21] Laroui, Hamed et al. "Nanotechnology in diagnostics and therapeutics for gastrointestinal disorders." *Digestive and liver disease : official journal of the Italian Society of Gastroenterology and the Italian Association for the Study of the Liver* vol. 45,12 (2013): 9951002. doi:10.1016/j.dld.2013.03.019
- [22] Dubey, R., Rajesh, Y. and More, M., 2015. Synthesis and Characterization of SiO₂ Nanoparticles via Sol-gel Method for Industrial Applications. *Materials Today: Proceedings*, 2(4-5), pp.3575-3579.
- [23] Sriramulu, D., Reed, E., Annamalai, M. *et al.* Synthesis and Characterization of Superhydrophobic, Self-cleaning NIR-reflective Silica Nanoparticles. *Sci Rep* **6**, 35993 (2016).
- [24] Ciucă, A., Grecu, C., Rotărescu, P., Gheorghe, I., Bolocan, A., Grumezescu, A., Holban, A. and Andronescu, E., 2017. Nanostructures for drug delivery: pharmacokinetic and toxicological aspects. *Nanostructures for Drug Delivery*, pp.941-957.
- [25] Mironyuk, I., Gun'ko, V., Vasylyeva, H., Goncharuk, O., Tatarchuk, T., Mandzyuk, V., Bezruka, N. and Dmytrotsa, T., 2019. Effects of enhanced clusterization of water at a surface of partially silylated nanosilica on adsorption of cations and anions from aqueous media. *Microporous and Mesoporous Materials*, 277, pp.95-104.
- [26] *Langmuir* 2011, 27, 21, 12977–12984 Publication Date: August 30, 2011
- [27] Zulfiqar, U., Subhani, T. and Husain, S., 2016. Synthesis and characterization of silica nanoparticles from clay. *Journal of Asian Ceramic Societies*, 4(1), pp.91-96.
- [28] Amidon, G., Secreast, P. and Mudie, D., 2009. Particle, Powder, and Compact Characterization. *Developing Solid Oral Dosage Forms*, pp.163-186.
- [29] Titus, D., James Jebaseelan Samuel, E. and Roopan, S., 2019. Nanoparticle characterization techniques. *Green Synthesis, Characterization and Applications of Nanoparticles*, pp.303-319.
- [30] Sergeev, Yuri V., Monika B. Dolinska, and Paul T. Wingfield. "Thermodynamic analysis of weak protein interactions using sedimentation equilibrium." *Current protocols in protein science* 77.1 (2014): 20-13.
- [31] Afriza, D., W. H. Suriyah, and S. J. A. Ichwan. "In silico analysis of molecular interactions between the anti-apoptotic protein survivin and dentatin, nordentatin, and quercetin." *Journal of Physics: Conference Series*. Vol. 1073. No. 3. IOP Publishing, 2018.

-
- [32] Moss, Richard B., et al. "Efficacy and safety of ivacaftor in patients with cystic fibrosis who have an Arg117His-CFTR mutation: a double-blind, randomised controlled trial." *The Lancet Respiratory Medicine* 3.7 (2015): 524-533.
- [33] Pace, C. Nick, et al. "Contribution of hydrophobic interactions to protein stability." *Journal of molecular biology* 408.3 (2011): 514-528.